



## Full Length Article

## Effect of rubidium incorporation on the optical properties and intermixing in Mo/Si multilayer mirrors for EUV lithography applications

M. Saedi<sup>a,1,2</sup>, C. Sfiligoj<sup>a,2</sup>, J. Verhoeven<sup>a</sup>, J.W.M. Frenken<sup>a,\*</sup><sup>a</sup> Advanced Research Center for Nanolithography, Science Park 106, 1098 XG Amsterdam, the Netherlands

## ARTICLE INFO

## Keywords:

EUV reflectivity  
 Multilayer mirrors  
 Thermodynamic stability  
 Intermixing

## ABSTRACT

High reflectivity and long-term stability in multilayer mirrors (MLMs) are crucial for extreme ultraviolet (EUV) photolithography. The conventional base stack to reflect 13.5 nm light is a Mo/Si multilayer, which offers a maximum theoretical reflectivity of 75%. In practice, however, the efficiency of the mirror is strongly affected by intermixing between Mo and Si. Diffusion barriers have therefore been adopted, which nevertheless do not provide a perfect solution. In this work, we propose to suppress intermixing in Mo/Si MLMs by substituting the pure Si with a Si compound that can ensure higher thermodynamic stability, while simultaneously providing comparably high EUV theoretical reflectivity, with the net effect of increasing both reflectivity and lifetime. Our theoretical calculations show that rubidium silicide is the most promising material for this purpose. We estimate the optical and thermodynamic properties for each phase of rubidium silicide, and we show that Mo/Rb<sub>12</sub>Si<sub>17</sub> provides the highest theoretical reflectivity, while Mo/RbSi is the most thermodynamically stable. The suppression of intermixing in Mo/RbSi MLMs should lead to a maximum reflectivity at least 2% higher than the best Mo/Si MLMs, integrated with diffusion barriers. The proposed Mo/RbSi MLM solution has the potential to increase the total EUV lithography throughput by ~50%.

## 1. Introduction

Molybdenum and silicon (Mo/Si) multilayer mirrors (MLMs) are to date the most viable technology to construct the optics systems for extreme-ultraviolet lithography (EUVL). The choice of Mo and Si as materials for the bilayers is mainly motivated by their high optical contrast and their low absorption at the EUV wavelength of 13.5 nm, adopted by the semiconductor industry. For Mo/Si MLMs, a theoretical peak reflectivity of 75% can be calculated [1], but in practice the maximum efficiency that can be achieved is only 69.5% [2]. Given that in EUVL machines, 10 mirrors are used in series to project a pattern onto a wafer, this value for the reflectivity implies that at best only ~3% of the original radiation reaches the end-stage. Improving the reflectivity of each MLM by as little as 1% would lead to a ~15% increase in the total EUVL throughput, accelerating the production speed and reducing the costs. Much effort has therefore been devoted to the suppression of the effects responsible for the deficit in experimental reflectivity.

The primary factor for the reflectivity loss in Mo/Si MLMs is the intermixing between Mo and Si at the interface. Previous studies have

shown that the interface sharpness can be improved via grazing-incidence ion bombardment. This technique, however, is not capable of suppressing the tendency of the bilayer constituents to diffuse and form compounds.

For that purpose, ultra-thin diffusion barriers have been integrated in Mo/Si MLMs and an experimental reflectivity as high as 71% could be obtained [3,4,5]. This method, however, presents two major limitations that prevent higher performance from being achieved. First of all, the additional layers introduce unwanted absorption and reflections, and secondly, these films are too thin to entirely prevent intermixing between Mo and Si, particularly at elevated temperatures and under the load of power flux of photons and particles [6,7].

An alternative strategy to improve the quality of the interfaces in MLMs is to reduce the thermodynamic driving forces responsible for the intermixing, which can be achieved by substituting the pure bilayer constituents with compounds. Several studies have investigated the use of Mo-based materials [8,9], demonstrating that by using Mo<sub>2</sub>C or MoSi<sub>2</sub> instead of Mo the thermodynamic stability of the multilayer could be improved. Nevertheless, the experimental reflectivity of these mirrors remained lower than that of Mo/Si MLMs integrated with

\* Corresponding author.

E-mail address: [j.frenken@arcnl.nl](mailto:j.frenken@arcnl.nl) (J.W.M. Frenken).<sup>1</sup> Present address: Leiden Institute of Chemistry, Leiden University, Einsteinweg 55, 2333 CC Leiden, the Netherlands.<sup>2</sup> The first two authors contributed equally to the work published in this article.

diffusion barriers, due to inferior optical properties of the added elements.

To our knowledge, the use of Si compounds has not been investigated yet in the context of MLMs. In this work, we show that by introducing Rb in the Si layer an overall efficiency superior to current best Mo/Si MLMs integrated barriers can potentially be achieved. Braat and Singh [10] have already proposed the incorporation of Rb in the form of RbCl to the Si layer. However, we are the first to study  $Rb_mSi_n$  compounds and to highlight the effect of using Si-based materials to increase the thermodynamic stability in MLMs, via suppression of intermixing. The choice of rubidium silicide is the result of an extensive search of the optical properties of all elements in the periodic table that could form a compound with Si while maintaining their EUV reflectivity comparable to that of standard Mo/Si MLMs.

## 2. Rubidium as additive to silicon in Mo/Si multilayer mirrors

To improve the performance of Mo/Si MLMs, we scrutinized possible compounds of Si that could simultaneously provide high EUV theoretical reflectivity and reduce the intermixing with Mo. In this search, we first calculated the EUV reflectivity for several elements  $X$  of the periodic table. In Table 1, we report the materials giving the highest MLM peak reflectivity,  $Peak1$ , at a wavelength of 13.5 nm and normal incidence. The reflectivity was calculated using the software IMD [11], designed for modeling the optical properties of multilayers. In all calculations, we set the number of bilayers  $N = 100$ . We optimized the bilayer period,  $d = d_{Mo} + d_x$ , and the thickness fraction of Mo,  $\Gamma = d_{Mo}/d$ , so that, at the given wavelength, the reflectivity is maximal. The roughness  $\sigma$  was set to zero for all interfaces, corresponding to ideally flat and sharp interfaces. Since for the conventional EUVL sources (of the tin-based laser-produced plasma type) the peak of the emission spectrum around 13.5 nm is much broader than the full width at half maximum of a typical MLM reflectivity profile (see Supplementary Material) [12], not only the peak reflectivity is relevant in the context of maximizing the total EUVL throughput, but also the width of the reflectivity peak. For a single mirror, the integral of the reflectivity peak should thus be regarded as the more relevant quantity. We therefore included in Table 1 the quantities  $NrInt1$  - which represents the normalized integral for a single MLM - and  $NrInt10$  - which represents an optical system with 10 MLMs in series [13]. Note that the  $NrInt10$  value contains the effects of both peak height and width on the total throughput of the lithography machine. In our calculations, we aim to find the multilayer mirrors with the highest  $Peak1$ , as it provides

**Table 1**

Theoretical maximum reflectivities of Mo/ $X$  MLMs at 13.5 nm and normal incidence, with  $X$  an element of the periodic table, assuming perfectly sharp and smooth interfaces. Columns  $Peak1$ ,  $NrInt1$  and  $NrInt10$  respectively indicate the peak reflectivity of a single MLM, the normalized integrated reflectivity of a single MLM and that of 10 MLMs in series [13]. The mass density  $\rho$ , the multilayer period  $d$  and the Mo/ $X$  layer thickness ratio  $\Gamma$  are also listed. See Supplementary Material for the complete reflectivity profiles.

Mo/	MLM parameters			Reflectivity [%]		
	$\rho$ [g cm <sup>-3</sup> ]	$d$ [nm]	$\Gamma$	$Peak1$	$NrInt1$	$NrInt10$
Si	2.33	6.89	0.38	75.3	100	100
Rb	1.53	6.86	0.30	81.2	89.8	172.4
Be	1.85	6.92	0.36	74.3	86.9	74.3
Sr	2.64	6.94	0.36	74.2	83.2	68.7
K	0.86	6.94	0.40	71.2	92.0	53.5
Ba	3.51	6.98	0.51	66.1	107.5	28.8
La	6.16	6.97	0.47	64.9	98.5	24.6
Ca	1.55	8.00	0.60	58.6	70.5	6.3
Y	4.47	5.56	0.58	55.6	58.3	3.1
Pr	6.77	7.08	0.51	50.5	62.4	1.3
Li	0.53	7.09	0.54	47.8	69.3	0.9
Zr	6.52	7.07	0.45	44.7	34.9	0.2

the most substantial contribution to the throughput of EUV light after multiple reflections. As Table 1 illustrates, Mo/Rb MLMs show the highest peak reflectivity ( $Peak1 = 81.2\%$ ). Accordingly, their normalized integrated reflectivity after 10 consecutive reflections is the highest, and it is more than 70% higher than the theoretical  $NrInt10$  value for Mo/Si MLMs. Despite its superior optical properties, elemental Rb is not a practical option for EUVL, due to its low melting point (39.30 °C), high vapor pressure at room temperature ( $2.85 \times 10^{-5}$  Pa) and strong chemical reactivity. All other combinations in Table 1 perform worse than Mo/Si MLMs. For the scope of our work, however, material combinations with a theoretical reflectivity of at least 70%, such as Be, K, Sr and La, are interesting to be investigated as additives to the Si layer.

All the materials reported in Table 1 are known to react with Si and form various silicide phases, with the exception of beryllium [14]. Beryllium has been successfully used as a diffusion barrier between Mo and Si, leading to a record EUV reflectivity [5]. However, a hypothetical Be-Si mixture would be thermodynamically unstable and, hence, prone to spontaneous segregation. We therefore excluded such mixtures from our discussion.

From Table 1 we selected the elements  $X =$  rubidium (Rb), strontium (Sr), potassium (K), and lanthanum (La), which have the highest  $NrInt10$  values in their chemical groups. For the silicides of these elements, we calculated the reflectivities of the corresponding Mo/ $X_nSi_m$  MLMs. In these calculations, we assumed all interfaces to be perfectly sharp and flat and we took the densities of  $X_nSi_m$  films from their crystalline forms, acquired from X-ray diffraction measurements. As shown in Table 2, most Mo/ $X_nSi_m$  MLMs give lower theoretical peak reflectivities than the best thinkable Mo/Si MLM, and all of them give lower integrated reflectivities. The fact that Mo/Rb $_nSi_m$  shows a theoretical reflectivity lower than Mo/Si - even though the reflectivity for Mo/Rb was higher (see Table 1) - should not come as a surprise. In fact, the EUV reflectivity is the highest when the absorption coefficients of the bilayer constituents are minimal, and the optical contrast between the two is maximal. Defining the complex refractive index as  $n = 1 - \delta + i\beta$ , in order to achieve the greatest refractive index contrast at the interfaces with Mo, we should thus substitute Si by a material for which the optical constants  $\delta$  and  $\beta$  are as low as possible. Note that a low value of  $\beta$  is also favorable for minimizing the absorption. In the EUV regime, the refractive index  $n$  of a compound can be approximated as a linear combination of the real and imaginary atomic scattering factors of its elemental constituents  $f_{1j}$  and  $f_{2j}$  [11]:

**Table 2**

Theoretical maximum reflectivity of Mo/ $XSi$  MLMs at 13.5 nm and normal incidence, with  $X =$  Rb, Sr, K and La, assuming perfectly sharp and flat interfaces. Columns  $Peak1$ ,  $NrInt1$  and  $NrInt10$  respectively indicate the peak reflectivity of a single MLM, the normalized integrated reflectivity of a single MLM and that of 10 MLMs in series [13]. The mass density  $\rho$ , the multilayer period  $d$  and the Mo/ $X$  layer thickness ratio  $\Gamma$  are also listed. See Supplementary Material for the complete reflectivity profiles.

Mo/	MLM parameters			Reflectivity [%]		
	$\rho$ [gr cm <sup>-3</sup> ]	$d$ [nm]	$\Gamma$	$Peak1$	$NrInt1$	$NrInt10$
Si	2.33	6.89	0.38	75.3	100	100
RbSi	2.72 [15]	6.92	0.36	74.9	89.4	82.7
Rb <sub>12</sub> Si <sub>17</sub>	2.53 [16]	6.91	0.36	75.6	91.5	92.4
Rb <sub>6</sub> Si <sub>46</sub>	2.76 [17]	6.91	0.38	73.9	95.1	79.6
Sr <sub>2</sub> Si	3.40 [18]	6.97	0.39	70.4	80.4	41.0
SrSi	3.50 [18]	6.97	0.39	70.1	81.8	40.0
SrSi <sub>2</sub>	3.42 [18]	6.96	0.4	70.6	85.7	45.3
KSi	1.78 [15]	6.99	0.44	66.0	86.2	24.5
K <sub>12</sub> Si <sub>17</sub>	1.76 [17]	6.97	0.43	67.8	89.2	32.9
K <sub>8</sub> Si <sub>46</sub>	2.46 [19]	6.94	0.42	69.6	92.8	44.0
La <sub>5</sub> Si <sub>3</sub>	5.75 [20]	6.98	0.47	64.3	91.1	20.5
LaSi	5.10 [20]	6.97	0.45	66.0	93.1	26.9
LaSi <sub>2</sub>	5.04 [20]	6.97	0.45	66.2	93.2	27.8

$$n = 1 - \frac{r_0 \lambda^2 \rho N_A \sum_j x_j (f_{1j} - if_{2j})}{2\pi \sum_j x_j M_j} \quad (1)$$

Here,  $r_0 = \frac{e^2}{4\pi\epsilon_0 m_e c^2}$  is the classical electron radius,  $\lambda$ , the wavelength, and  $N_A$ , the Avogadro's number. We chose an expression of the refractive index in which the mass density of the compound,  $\rho$ , appears explicitly, together with the molar masses  $M_j$  and compositional fractions  $x_j$  of the constituents.

Tables 1 and 2 show that the density of  $Rb_nSi_m$  is greater than that of either Rb or Si. From Eq. (1), we see that this makes the refractive index of the silicide deviate further from unity, reducing the optical contrast with Mo. In turn, the EUV reflectivity of the silicide-based MLM becomes lower than that of Mo/Si.

For the same reason, also for K and Sr, the theoretical reflectivity values of the corresponding  $Mo/X_nSi_m$  MLMs are lower than those of  $Mo/X$  MLMs. By contrast,  $Mo/LaSi_2$  and  $Mo/LaSi_2$  show higher reflectivities than  $Mo/La$ , as their densities are lower than that of  $La$ .

As mentioned before, the replacement of the Si layer with a silicide is motivated by a reduction in thermodynamic driving force towards intermixing. If the intermixing is suppressed sufficiently, a  $Mo/X_nSi_m$  MLM could in principle reach a reflectivity higher than the current best  $Mo/Si$  MLM integrated with diffusion barriers. This is suggested in Table 2, in particular for three  $Mo/Rb_nSi_m$  MLMs with different silicide compositions. We therefore focus the remainder of our discussion on the  $Mo/Rb_nSi_m$  system.

Literature on the properties of rubidium silicide is rather scarce. Two main equilibrium crystal structures are known, depending on the concentration of Rb. The clathrate phase (Rb content < 10% at.) consists of  $Rb^{+1}$  cations, encapsulated in  $Si_{20}$ ,  $Si_{24}$  or  $Si_{28}$  cages [19,21]. The Zintl phase (Rb content 40–50 at. %) consists of  $Si_4^{-4}$  or  $Si_9^{-4}$  Zintl clusters, surrounded by  $Rb^{+1}$  cations [15,16]. The clathrate phase,  $Rb_6Si_{46}$ , and the two Zintl phases,  $RbSi$  (also known as  $Rb_4Si_4$ ) and  $Rb_{12}Si_{17}$ , are the most common ones.

In either phase,  $Rb_nSi_m$  presents several favorable properties over elemental Rb. First of all, the decomposition temperatures of  $Rb_6Si_{46}$  and  $RbSi$  are reported to be 803 K [21] and 623 K [22] respectively, which are considerably higher than the melting point of Rb. Secondly, while Rb violently reacts with air, the clathrate phase is reported to be as stable as pure silicon [21]. The two Zintl phases are reported to be highly unstable in contact with air [22]. However, this would not render their application in EUVL impractical since capping layers could be used to separate them from the ambient. In addition, EUV MLMs are fabricated and operated under vacuum conditions. Therefore, by implementing proper preparation and handling procedures, all  $Mo/Rb_nSi_m$  combinations included in Table 2 could constitute valid options for EUV lithography.

In our study, we assume the silicide phases to be in a crystalline form. However, typical layers of as-deposited EUV MLMs are amorphous or polycrystalline. Although in the EUV regime the optical constants of a material can be assumed to be independent of the relative arrangements of its atoms, the mass densities  $\rho$  of amorphous phases are usually somewhat lower than their ideal crystalline counterparts. For example, the density of amorphous Si is 1.8% less than that of crystalline Si [23]. As discussed above, a decrease in density would lead to an enhanced reflectivity (see Equation (1)). Using the IMD software, we calculated that a 2% reduction in the density of  $RbSi$  from its crystalline value of  $2.72 \text{ g cm}^{-3}$  would increase the *Peak1* reflectivity of  $Mo/RbSi$  by approximately 0.25%. Despite this favorable contribution, for the remaining of our analysis we will disregard the effect of density deviations since it is expected to be modest in comparison with the other factors (e.g. suppression of intermixing).

In the following sections we give estimates for  $Rb_nSi_m$  of the optical constants, the thermodynamic stability and the reflectivity of  $Rb_nSi_m/Mo$  MLMs.

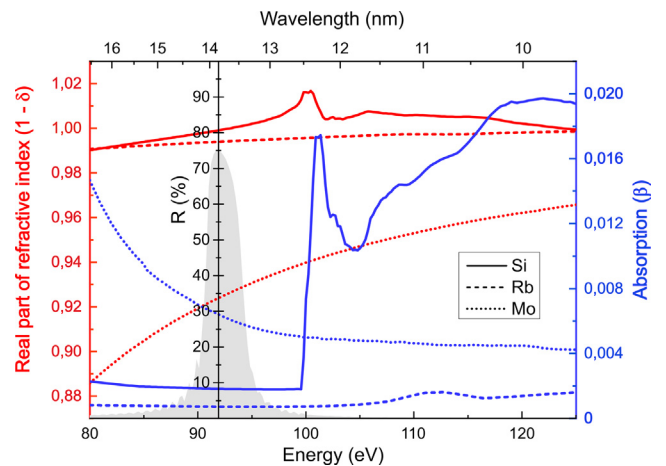


Fig. 1. Real (red) and imaginary component (blue) of the index of refraction in the vicinity of 13.5 nm (91.8 eV), for Si (solid lines), Rb (dashed lines) and Mo (dotted lines). The gray area represents the calculated reflectivity profile of a single  $Mo/Rb_nSi_m$  MLM.

### 2.1. EUV optical properties of rubidium silicide

In Fig. 1 we show the complex index of refraction as a function of photon energy for the three materials of interest - Mo, Si, and Rb. The real ( $1 - \delta$ ) and imaginary component ( $\beta$ ) are represented in red and blue respectively, and have been calculated using reference [24]. The optical properties of the Rb and Si atoms in the silicide however are not the same as those in the individual elements. In fact, when a compound is formed, it is known that the electronic energy levels of the constituent atoms are shifted [25]. Even though this chemical shift is usually ignored (as in Eq. (1)) the scattering factors which determine the optical properties of the compound can be strongly affected. In what follows we explore the effect of the chemical shift on the EUV reflectivity in  $Mo/Rb_nSi_m$  MLMs.

In the case of  $Rb_nSi_m$ , the chemical shift undergone by Si is expected to be negative, as the low electronegativity of Rb - one of the lowest in the periodic table - negatively charges the Si atoms. In turn, by looking at Fig. 1, we see that a translation of the optical spectra towards lower values leads to an increase in the refractive index of Si (red solid line) at the EUV energy of 91.8 eV. Hence, the optical contrast between  $Rb_nSi_m$  and Mo becomes slightly higher than what predicted by Equation (1), thereby contributing to a raise in reflectivity.

The absorption coefficient of Si (blue solid line in Fig. 1), on the other hand, stays practically unchanged, provided that the chemical shift is not large enough that the adsorption edge at 100 eV enters into the EUV reflectivity window of the MLM (depicted in gray in Fig. 1).

The precise magnitude of the chemical shift in Si depends on the spatial arrangement of the atoms and the nature of the chemical bonds within the silicide. Qualitatively, the shift of the absorption edge is proportional to the effective charge of the absorbing ions, following Suchet's empirical rule [26]. Using this rule, we can calculate for Si a chemical shift of approximately  $-1.0 \text{ eV}$  (see [Supplementary Material](#) for further details on the calculations).

We note that Suchet's rule does not take into account the detailed bonding characteristics or the crystal structure of the compound [26], which might influence the chemical shift, as for the case of rubidium silicide in the Zintl phase. Here, the Si atoms - forming  $Si_4^{-4}$  tetrahedral clusters - have an electric charge of  $-4$  on 4 closely packed Si atoms. Therefore, the negative electric field and, accordingly, the effective negative charge contributing to the chemical shift are expected to increase. For an accurate determination of the energy shift induced by this effect, synchrotron X-ray absorption measurements would be necessary, as the precise atomic geometry of a freshly deposited  $Rb_nSi_m$  film is not known. However, we predict that the refractive index and,

thus, the EUV reflectivity could increase even further.

In the case of Rb, we do not have sufficient information to calculate the chemical shift. However, its sign is expected to be positive and to have a negligible effect on the scattering factors of Rb in the silicide, as they are nearly constant around 13.5 nm.

To estimate the effect of the chemical shift of Si on the reflectivity of Mo/Rb<sub>n</sub>Si<sub>m</sub> MLMs, we recalculated the theoretical reflectivity substituting the original Si optical constants with those shifted by  $-1.0$  eV. For Mo/RbSi MLMs, for example, this correction leads to an increase in *Peak1*, *NrInt1*, and *NrInt10* of 0.02%, 0.27%, and 0.58%, respectively.

Since the chemical shift has a modest impact on the MLM reflectivity with respect to other factors (such as suppression of intermixing or density variations), we will neglect it in the following analysis. However, our results suggest that the addition of Rb and the special arrangement of Si atoms in the Zintl phase have the potential to result in a noticeable enhancement of reflectivity in EUVL optics, via the chemical shift of the electronic states of the Si atoms.

## 2.2. Intermixing in molybdenum/rubidium silicide multilayers

It is known that the measured reflectivities of EUV MLMs are lower than the theoretical values and that they decrease over time and with increased operation temperature. This is due to the non-ideal quality of the interfaces in the multilayer stack; sharp, non-equilibrium interfaces tend to lower their free energy by becoming intermixed and roughened through diffusion and compound formation. This process is driven by thermodynamics and mostly by the (negative) change in free energy  $\Delta G_r = \Delta H_r - T\Delta S_r$  due to compound formation. Here,  $\Delta H_r$  and  $\Delta S_r$  are the reaction enthalpy and entropy, respectively. Since in solid-state reactions, entropy changes are often orders of magnitude smaller than enthalpy changes [27], we will neglect  $\Delta S_r$ . We therefore approximate the free energy change due to the formation of a compound as  $\Delta G_r \approx \Delta H_r$ . When the MLM is not protected by diffusion barriers, compound formation will continue, in principle, until the entire stack is turned into a, single, homogeneous mixture. In practice, the mixed interfaces have widths of several atomic layers to several nanometers.

For completeness, we should mention that there is an additional thermodynamic driving force for interface mixing, deriving from the reduction of the interfacial free energy. This effect has a short-range character and would, by itself, lead to interface widths in the order of one or just a few atomic layers [28]. As this interface-energy effect is bound to be modest compared to the enthalpy effect, we leave it out of our analysis.

Next to thermodynamics, also kinetics plays an essential role in determining the rate of intermixing. For a lack of detailed information, here we simply assume that we should not expect essential differences in diffusion coefficients between the materials that we address. Instead, we entirely base our predictions of the interface widths in Mo/Rb<sub>n</sub>Si<sub>m</sub> MLMs on the differences in the enthalpies of compound formation.

In agreement with the above considerations, it has been shown experimentally that the roughness in Mo/Si MLMs is mainly caused by silicide formation [29,30]. The three possible molybdenum silicide phases are Mo<sub>3</sub>Si, Mo<sub>5</sub>Si<sub>3</sub> and MoSi<sub>2</sub> [31].

For the case of Mo/Rb<sub>n</sub>Si<sub>m</sub> MLMs, interdiffusion and compound formation between Rb and Mo can be excluded, as they are mutually insoluble at room temperature and do not form any intermetallic phase [32]. So, similar to the Mo/Si MLMs, also for Mo/Rb<sub>n</sub>Si<sub>m</sub> MLMs, molybdenum silicides are the main product of intermixing.

Using the reaction equations specified in the *Supplementary Material*, we calculated the enthalpies of formation for one mole of atoms for each molybdenum silicide phase (see Table 3), both in the case of Mo/Si and Mo/RbSi MLMs.

Table 3 shows that for Mo/Rb<sub>n</sub>Si<sub>m</sub> MLMs, where the Si atoms have already reacted with the Rb atoms, the thermodynamic driving force for the formation of Mo<sub>n</sub>Si<sub>m</sub> is significantly decreased, by 82% for Mo<sub>3</sub>Si and 92% for Mo<sub>5</sub>Si<sub>3</sub>. The enthalpy of formation of MoSi<sub>2</sub> even turns

**Table 3**

Formation enthalpies of three Mo<sub>n</sub>Si<sub>m</sub> compounds in Mo/Si MLMs (second column) and Mo/RbSi MLMs (third column).

Compound	$\Delta H_f$ (kJ) in Mo/Si MLMs	$\Delta H_f$ (kJ) in Mo/RbSi MLMs
Mo <sub>3</sub> Si	$-30.5 \pm 1.5$	$-5.6 \pm 2.3$
Mo <sub>5</sub> Si <sub>3</sub>	$-39.2 \pm 1.5$	$-2.8 \pm 2.5$
MoSi <sub>2</sub>	$-45.3 \pm 1.5$	$+10.6 \pm 3.0$

positive, which corresponds to full, thermodynamic protection against the formation of that silicide in Mo/RbSi MLMs.

As Rb in the silicide phase is in the +1 oxidation state, the higher the Rb content the more positive is the enthalpy of Mo<sub>n</sub>Si<sub>m</sub> formation. Therefore, in the sequence RbSi (50.0 at.% Rb), Rb<sub>12</sub>Si<sub>17</sub> (41.4 at.% Rb) and Rb<sub>6</sub>Si<sub>46</sub> (11.5 at.% Rb), the first one will provide the best protection against the formation of Mo<sub>n</sub>Si<sub>m</sub>. For this reason, in the following discussion we will focus only on Mo/RbSi MLMs. However, we note that since Mo/Rb<sub>12</sub>Si<sub>17</sub> gives a higher theoretical reflectivity than RbSi (see Table 2), the optimum rubidium silicide composition might not be RbSi and it should be addressed experimentally.

The suppression of Mo<sub>n</sub>Si<sub>m</sub> formation in Mo/RbSi multilayer mirrors should lead to sharper interfaces and therefore to an EUV reflectivity closer to the theoretical value. In order to quantify the expected reflectivity, we now proceed to associate the calculated enthalpies with expectations for the interface thickness.

We begin by calculating the interface width in Mo/Si MLMs. The theoretical reflectivity matches the maximum experimental value for such mirrors of 69.5% when we introduce in our numerical model an interface width of  $\sigma = 0.71$  nm (see Table 4). This value for  $\sigma$  is comparable to the thickness of intermixed regions observed with TEM [33,34].

In order to predict the reduction in intermixing in Mo/RbSi MLMs, we then use the approximation that the reduction in the width of the intermixed region in Mo/RbSi MLMs would simply scale proportionally to the suppression of the Mo<sub>n</sub>Si<sub>m</sub> formation enthalpies. We note that this method actually underestimates the suppression of the interface width in Mo/RbSi. More realistic would be to expect changes in the activation energy for interdiffusion to scale linearly with changes in the enthalpy for compound formation. As the activation energy appears in the exponential factor that governs the interdiffusion rate, a super-linear effect should be expected on the interface width. A second conservative estimate is introduced by our choice to concentrate in the remainder of this article on the weakest reduction in the enthalpy for compound formation (see Table 3), namely that of 82% with respect to Mo<sub>3</sub>Si.

In addition to the enthalpy-driven intermixing, we also take into account the contributions to the width of all interfaces deriving from the initial roughness of the substrate and from the kinetics of the deposition process. AFM experiments have shown that the roughness levels of the individual layers in the MLM can be lowered down to 0.1 nm rms by ion polishing [1]. As a conservative estimate, we added a roughness of 0.2 nm to all interfaces in our calculations, including the substrate surface and the surface of the top layer.

We thus estimate that a suppression of intermixing of 82% would lead to an interface width in Mo/Rb<sub>n</sub>Si<sub>m</sub> of  $\sigma \approx 0.71 - (0.71 - 0.20) \times 82\% \text{ nm} = 0.29 \text{ nm}$ .

In Table 4 we report the values calculated for the reflectivity for a Mo/RbSi MLM, including  $\sigma = 0.29$  nm (second line) to the ideal multilayer structure. We also explored the result for the case that the suppression of intermixing were a factor 2 more modest (only 41% suppression of the intermixing in Mo/RbSi compared to Mo/Si), corresponding to  $\sigma = 0.5$  nm (third line).

**Table 4**

Calculated maximum achievable reflectivities for Mo/Si, Mo/RbSi and Mo/Si/B<sub>4</sub>C MLMs, at 13.5 nm and normal incidence. The choices for the interface width  $\sigma$  are discussed in the text. The columns *Peak1*, *NrInt1* and *NrInt10* indicate respectively the peak reflectivity of a single MLM, and the normalized integrated reflectivities of a single MLM and a combination of 10 MLMs in series [13]. See *Supplementary Material* for the complete reflectivity profiles.

Mo/	MLM parameters					Reflectivity [%]		
	Interlayer	$\sigma$ [nm]	$\rho$ [gr cm <sup>-3</sup> ]	$d$ [nm]	$\Gamma$	<i>Peak1</i>	<i>NrInt1</i>	<i>NrInt10</i>
Si	None	0.71	2.33	6.92	0.38	69.5 [1]	100	100
RbSi	None	0.29	2.72 [15]	6.92	0.36	73.9	112.1	200.9
RbSi	None	0.50	2.72 [15]	6.92	0.36	71.9	102.6	141.3
Si	B <sub>4</sub> C [0.30 nm]	0.57	2.33	6.92	0.35	70.15 [3]	110.0	128.6

### 3. Results and discussion

Table 4 summarizes our estimates for the interface width in Mo/RbSi MLMs and the corresponding values of the EUV reflectivity. As before, we optimized the periodicity  $d$  and the bilayer thickness ratio  $\Gamma$  in order to reach the highest possible peak reflectivity *Peak1*. For all cases, the number of MLM periods was  $N = 100$  and the interface widths of the substrate and top surfaces were set to  $\sigma = 0.2$  nm. For all other interfaces we used  $\sigma = 0.29$  nm (or  $\sigma = 0.5$  nm, assuming half the suppression of intermixing). In Table 4 we also include the normalized integral reflectivities for a single mirror *NrInt1* and for a series of ten mirrors, *NrInt10*. For reference, we show the corresponding numbers for a Mo/Si MLM [1] (first line in Table 4) and for the type of mirror currently employed in EUV lithography machines, i.e. a Mo/Si MLM with B<sub>4</sub>C diffusion barriers [3]. For these two reference systems, we used the experimental values of the peak reflectivity to fit the interface width and subsequently calculated the other MLM properties. As previously mentioned, the theoretical reflectivity matches the experimental value in Mo/Si MLMs when we set  $\sigma$  to 0.71 nm for all Mo-Si interfaces. For Mo/Si MLMs with 0.30 nm thick B<sub>4</sub>C interlayers, separating the Mo layers from the Si layers, we have to assume an effective  $\sigma = 0.57$  nm for all B<sub>4</sub>C-mediated Mo/Si interfaces, in order to match the experimentally reported reflectivity.

As Table 4 illustrates, the reflectivity performance expected for Rb-based mirrors is far superior to that of Mo/Si MLMs and that of Mo/Si MLMs integrated with B<sub>4</sub>C barrier layers, even if we assume the more modest suppression of the intermixing, corresponding to  $\sigma = 0.50$  nm.

What we clearly recognize is that the *NrInt1*-values reflect not only the changes in the peak reflectivity, but also in the width of the reflectivity spectrum. On the other hand the *NrInt10*-values vary much more strongly with the peak reflectivity because this effect is factored in 10 times. Comparing the normalized, integrated reflectivities of 10 mirrors in series (*NrInt10*), we see that the Mo/RbSi MLMs with the sharpest interfaces can in principle reach a reflectivity that is 56% higher (200.9% instead of 128.6%) than Mo/Si MLMs integrated with B<sub>4</sub>C diffusion barriers.

Regarding the feasibility of implementation of these mirrors in EUV lithography technology, some additional considerations are relevant. First of all, Rb-based mirrors should be operated well below their decomposition temperatures. In current EUVL optics, the mirror closest to the EUV light source – the collector mirror – reaches temperatures of 400–500 K during operation; the other MLMs – constituting the illuminator and projection optical stages – are subjected to progressively lower temperatures. As previously stated, the decomposition temperature of RbSi is 623 K [21], which would therefore not restrict its application for EUVL. However, as the EUV source power continues to be raised, the collector mirror temperature may become a future point of concern in this respect.

Another important factor is that in current EUVL machines with sources of EUV light based on laser-produced tin plasma, the MLMs are operated in a hydrogen-rich environment, with a H<sub>2</sub> partial pressure in the order of 5 Pa. The hydrogen serves to mitigate the effect of tin in these machines and avoid and/or counteract contamination by tin of

the EUV optics. In combination with the intense EUV light, this puts the MLMs in contact not only with H<sub>2</sub> gas, but also with H<sup>+</sup> ions and H radicals, which are known to lead to degradation (e.g. blistering [35]) of Mo/Si MLMs. While a Mo/RbSi MLM would be stable under vacuum conditions, in a hydrogen environment, RbSi may absorb hydrogen and eventually even form RbH and RbSiH<sub>3</sub>. This could potentially lead to a significant volume expansion and increase of the EUV wavelength at which the reflectivity of the MLM peaks, which should be regarded as a form of degradation of this type of MLM. Rb-based MLMs should therefore have to be adequately protected from hydrogen incorporation with suitable capping layers. It has been already shown however that implanting the Si layer with low energy (150 eV) hydrogen ions leads to a significant reflectivity enhancement in Mo/Si MLMs [36]. MLMs based on hydrogenated rubidium or hydrogenated rubidium silicide, if appropriately designed for reflecting 13.5 nm light may therefore constitute a potential route for enhancing the MLM reflectivity even further.

In the context of the experimental realization of the proposed MLM structures, we have not found information in the literature about the deposition of Rb compounds. We expect that it should be possible to use techniques such as sputter-deposition and pulsed-laser-deposition for this purpose, which are both applied for the deposition of complex compound materials. In addition to deposition experiments, aiming to implement the proposed Mo/RbSi multilayer structure, measurements need to be carried out to verify the predicted EUV-reflectivity properties and to verify the predicted stability of the structure at elevated temperatures.

### 4. Conclusion

In the search for new ways to improve the reflectivity and stability of Mo/Si-type multilayer EUV mirrors, we explored new multilayer structures, consisting of bilayers of molybdenum and silicon-based compounds. We aimed for material combinations with high optical contrast and minimal absorption around 13.5 nm, and with a minimal thermodynamic driving force for intermixing at the interfaces. Our numerical calculations have shown that, among the various considered material combinations, Mo/Rb<sub>m</sub>Si<sub>n</sub> provides the highest theoretical reflectivity in the spectral regime 12.5–14.5 nm. The favorable optical properties of Rb, the chemical shift in Si induced by the formation of a compound with Rb, and the thermodynamic suppression of intermixing at the Mo/Rb<sub>m</sub>Si<sub>n</sub> interfaces are all argued to contribute to enhancements in reflectivity and stability of these MLMs, with a calculated reflectivity exceeding by more than 2% that of the current best Mo/Si MLMs, integrated with diffusion barriers. This result is expected to increase the EUV throughput of a 10-mirror system by more than 50% [37]. We believe that this research represents a new approach for the design and optimization of EUV multilayer mirrors, which may be relevant for future generations of projection lithography tools.

### CRedit authorship contribution statement

M. Saedi: Conceptualization, Methodology, Writing - original draft.

**C. Sfiligoj:** Conceptualization, Writing - original draft, Writing - review & editing. **J. Verhoeven:** Supervision. **J.W.M. Frenken:** Supervision, Writing - review & editing.

### Declaration of Competing Interest

The authors declare that they have no known competing financial interests or personal relationships that could have appeared to influence the work reported in this paper.

### Acknowledgments

This work has been carried out at ARCNL, a public-private partnership of the University of Amsterdam (UvA), the VU University Amsterdam, The Dutch Research Council (NWO) and the semiconductor equipment manufacturer ASML.

### Appendix A. Supplementary material

Supplementary data to this article can be found online at <https://doi.org/10.1016/j.apsusc.2019.144951>.

### References

- [1] E. Louis, A.E. Yakshin, T. Tsarfati, F. Bijkerk, Nanometer interface and materials control for multilayer EUV-optical applications, *Prog. Surf. Sci.* 86 (2011) 255–294.
- [2] E. Louis, A.E. Yakshin, P.C. Görts, S. Oestreich, R. Stuik, M.J.H. Kessels, E.L.G. Maas, F. Bijkerk, M. Haidl, S. Muellender, M. Mertin, D. Schmitz, F. Scholze, G. Ulm, Progress in Mo/Si multilayer coating technology for EUVL optics, *Proc. SPIE* 3997 (2000) 406–411.
- [3] A.E. Yakshin, R.W.E. van de Kruijs, I. Nedelcu, E. Zoethout, E. Louis, F. Bijkerk, H. Enkisch, S. Muellender, Enhanced reflectance of interface engineered Mo/Si multilayers produced by thermal particle deposition, *Proc. SPIE* 6517 (2007) 65170.
- [4] J. Bosgra, E. Zoethout, A.M.J. van der Eerden, F. Boekhout, J. Verhoeven, R.W.E. van de Kruijs, A.E. Yakshin, F. Bijkerk, Structural properties of sub-nanometer thick Y layers in extreme ultraviolet multilayer mirrors, *Appl. Opt.* 51 (2012) 8541–8548.
- [5] N.I. Chkhalo, S.A. Gusev, A.N. Nechay, D.E. Pariev, V.N. Polkovnikov, N.N. Salashchenko, F. Schäfers, M.G. Sertsu, A. Sokolov, M.V. Svechnikov, D.A. Tatarsky, High-reflection Mo/Be/Si multilayers for EUV lithography, *Opt. Lett.* 42 (24) (2017) 5070–5073.
- [6] V.V. Kondratenko, Yu.P. Pershin, O.V. Poltseva, A.I. Fedorenko, E.N. Zubarev, S.A. Yulin, I.V. Kozevnikov, S.I. Sagitov, V.A. Chirkov, V.E. Levashov, A.V. Vinogradov, Thermal stability of soft X-Ray Mo-Si and MoSi<sub>2</sub>-Si multilayer mirrors, *Appl. Opt.* 32 (10) (1993) 1811–1816.
- [7] H. Takenaka, T. Kawamura, Thermal stability of Mo/C/Si/C Multilayer Soft X-ray Mirrors, *J. Electron Spectrosc. Relat. Phenom.* 80 (1996) 381–384.
- [8] T. Feigl, S.A. Yulin, N. Kaiser, R. Thielsch, Magnetron sputtered EUV mirrors with high-thermal stability, *Proc. SPIE* 3997, Emerging Lithographic Technologies IV vol. 420, (2000).
- [9] A.I. Fedorenko, V.V. Kondratenko, L.S. Palatnik, S.A. Yulin, E.N. Zubarev, V.P. Nikitskiy, S.B. Ryabukha, Space test of Mo-Si, MoSi<sub>2</sub>-Si, W-Si, and WSi<sub>2</sub>-Si x-ray multilayer mirrors on the Russian orbital station Mir, *Proc. SPIE* 2453, X-Ray Optics and Surface Science, 1995, p. 11.
- [10] M. Singh, J.M. Braat, Design of multilayer extreme-ultraviolet mirrors for enhanced reflectivity, *Appl. Opt.* 39 (2000) 2189.
- [11] D.L. Windt, IMD—Software for modeling the optical properties of multilayer films, *Comput. Phys.* 12 (1998) 360–370.
- [12] J.R. Hoffman, A.N. Bykanov, O.V. Khodykin, A.I. Ershov, N.R. Böwering, I.V. Fomenkov, W.N. Partlo, D.W. Myers, LPP EUV conversion efficiency optimization, *Proc. SPIE* 5751, Emerging Lithographic Technologies IX, 2005, p. 892.
- [13] The integral reflectivity values are all normalized to that of Mo/Si MLMs in the 12.5–14.5 nm spectral range. The values for integral reflectivities for a single MLM and for a combination of 10 consecutive MLMs are respectively: 48.9 and 1.68 (in units of %·nm), for Mo/Si MLMs with ideally sharp and flat interfaces (see Table 1 and 2); these values drop to 37.6 and 0.584 (in units of %·nm) for Mo/Si MLMs with modest interfacial diffuseness (see Table 3).
- [14] H. Okamoto, Be-Si (Beryllium-Silicon), *J. Phase Equilibria Diffusion* 30 (115) (2009) 1547–7037.
- [15] H.G. von Schnering, M. Schwarz, J.-H. Chang, K. Peters, E.-M. Peters, R. Nesper, Refinement of the crystal structures of the tetrahedrotetrasilicides K<sub>4</sub>Si<sub>4</sub>, Rb<sub>4</sub>Si<sub>4</sub> and Cs<sub>4</sub>Si<sub>4</sub>, *Z. Kristallogr. NCS* 220 (2005) 525–527.
- [16] V. Quéneau, E. Todorov, S.C. Sevov, Synthesis and Structure of Isolated Silicon Clusters of Nine Atoms, *J. Am. Chem. Soc.* 120 (1998) 3263–3264.
- [17] C. Hoch, M. Wendorff, C. Röhr, Synthesis and crystal structure of the tetrelides A<sub>1</sub>2M<sub>1</sub>7 (A = Na, K, Rb, Cs; M = Si, Ge, Sn) and A<sub>4</sub>P<sub>6</sub>9 (A = K, Rb), *J. Alloy. Compd.* 361 (2003) 206–221.
- [18] A. Palenzona, M. Pani, The phase diagram of the Sr-Si system, *J. Alloy. Compd.* 373 (2004) 214–219.
- [19] G.K. Ramachandran, P.F. McMillan, K<sub>7,62(1)</sub>Si<sub>46</sub> and Rb<sub>6,15(2)</sub>Si<sub>46</sub>: two structure I clathrates with fully occupied framework sites, *J. Solid State Chem.* 154 (2000) 626–634.
- [20] M.V. Bulanova, P.N. Zheltov, K.A. Meleshevich, P.A. Saltykov, G. Effenberg, J.-C. Tedenac, Lanthanum-silicon system, *J. Alloy. Compd.* 329 (2001) 214–223.
- [21] C. Cros, M. Pouchard, P. Hagenmuller, Sur une nouvelle famille de Clathrates minéraux isotopes des hydrates de gaz et de liquides. Interprétation des résultats obtenus, *J. Solid State Chem.* 2 (1970) 570–581.
- [22] E. Hohman, Silicide und Germanide der alkalimetalle, *Z. Anorg. Allg. Chem.* 257 (1948) 113.
- [23] J.S. Custer, M.O. Thompson, D.C. Jacobson, J.M. Poate, S. Roorda, W.C. Sinke, F. Spaepen, Density of amorphous Si, *Appl. Phys. Lett.* 64 (1994) 437.
- [24] B.L. Henke, E.M. Gullikson, J.C. Davis, AtDataNucDataTable93 “X-Ray interactions: photoabsorption, scattering, transmission, and reflection at E = 50–30,000 eV, Z = 1–92”, Atomic Data and, Nuclear Tables 54 (1993) 181–342.
- [25] K. Siegbahn, Electron spectroscopy for chemical analysis (E.S.C.A.), *Phil. Trans. Roy. Soc. Lond.* 268 (1970) 33–57.
- [26] M.N. Ghatikar, B.D. Padalia, R.M. Nayak, Chemical shifts and effective charges in ternary and complex systems, *J. Phys. C: Solid State Phys.* 10 (1977) 4173–4180.
- [27] F.R. de Boer, R. Boom, W.C.M. Mattens, A.R. Miedema, A.K. Niessen, Cohesion in metals: transition metal alloys, North-Holland Physics Publishing, Amsterdam, 1988.
- [28] B.M. Clemens, W.D. Nix, V. Ramaswamy, Surface-energy-driven intermixing and its effect on the measurement of interface stress, *J. Appl. Phys.* 87 (2000) 2816.
- [29] V. Fokkema, Real-time Scanning Tunneling Microscopy Studies of Thin Film Deposition and Ion Erosion, Ph. D Thesis University of Leiden, The Netherlands, 2011.
- [30] I. Nedelcu, R.W.E. van de Kruijs, A.E. Yakshin, F. Bijkerk, Temperature dependent nanocrystal formation in Mo/Si multilayers, *Phys. Rev. B* 76 (24) (2007) 245404.
- [31] A.E. Yakshin, E. Louis, P.C. Görts, E.L.G. Maas, F. Bijkerk, Determination of the layered structure in Mo/Si multilayers by grazing incidence x-ray reflectivity, *Physica B – Condensed Matter* 283 (1–3) (2000) 143–148.
- [32] W. Moffatt, Mo-Rb, The Handbook of Binary Phase Diagrams, Genium Pub. Corp., USA, (1984) 3/82.
- [33] S. Yulin, T. Feigl, T. Kuhlmann, N. Kaiser, A.I. Fedorenko, V.V. Kondratenko, O.V. Poltseva, V.A. Sevryukova, A.Yu. Zolotaryov, E.N. Zubarev, Interlayer transition zones in Mo/Si superlattices, *J. Appl. Phys.* 92 (2002) 1216.
- [34] I. Nedelcu, R.W.E. van de Kruijs, A.E. Yakshin, F. Bijkerk, Thermally enhanced interdiffusion in Mo/So multilayers, *J. Appl. Phys.* 103 (8) (2008) 083549.
- [35] A.S. Kuznetsov, M.A. Gleeson, F. Bijkerk, Hydrogen-induced blistering mechanisms in thin film coatings, *J. Phys.: Condens. Matter*, 24(5) (2012) 052203.
- [36] R. Schlattmann, A. Keppel, Y. Xue, J. Verhoeven, Enhanced reflectivity of soft X-ray multilayer mirrors by reduction of Si atomic density, *Appl. Phys. Lett.* 63 (24) (1993) 3297–3299.
- [37] The work described in this article forms the basis of Patent. Nr. WO2017076694A1, entitled “Multilayer reflector, method of manufacturing a multilayer reflector and lithographic apparatus”.